

## Manipulation of particles using dielectrophoresis in a microchannel

Eugen CHIRIAC<sup>1,2</sup>, Marioara AVRAM<sup>1</sup>, and Corneliu BĂLAN<sup>2</sup>

<sup>1</sup>National Institute for R&D in Microtechnologies – IMT Bucharest

<sup>2</sup>Politehnica University of Bucharest, REOROM Laboratory

E-mails: eugen.chiriac@imt.ro, marioara.avram@imt.ro,  
corneliu.balan@upb.ro

**Abstract.** Over the years several methods were used to separate cells within a microfluidic device such as cavities, with vortex microfluidics method, or cell trapping mechanisms using size filters. However, one of the methods that is widely used to separate cancer cells from blood cells is the dielectrophoresis. In this work we employ the numerical code COMSOL Multiphysics for a dielectrophoretic separation of CTCs (circulating tumor cells) from RBCs (red blood cells) in a 3D microchannel. The microfluidic device is composed of one inlet and three outlets. The non-uniform alternative electric field is generated using interdigitated electrodes and it separates the cells within the device to the corresponding outlet. The electric field frequency was set to 100 kHz. For this paper, one single CTC line is selected MDA-MB-231, breast cancer cells. The CTCs and the RBCs are considered in an ideal way in the simulation as spheres, but with the afferent characteristics. This work can be extended to testing multiple CTC lines at various flow velocities and electric field frequencies

**Key-words:** particle manipulation, dielectrophoresis, microchannel, CFD.

### 1. Introduction

The process of particle separation has a significant importance in the medical field, biological, chemical, food industry and environment. The flowing regime in the microfluidic devices is usually laminar and this allows an accurate flow control and its prediction.

In a microchannel, particles can be separated through various methods: passive, active and combined [1]. The passive methods rely on the geometry of the microchannel, various obstacles in the flow field, accurate flow control and the interaction between particles and geometry [2], without the influence of external fields. The active methods require in general a simplistic geometry but use external fields of various types: electric [3], magnetic [4], acoustic [5] or optic [6, 7].

Dielectrophoresis is the phenomenon that controls the particles movement as a result of applying a gradient of electric field, which induces a dipole moment on the cells, which is due to the electrical polarizability of the cell membrane as it moves in a suspension medium. The cell is translocated in the electric field until it reaches an electrostatic equilibrium. This movement is due to the dielectrophoretic force ( $f_{DEP}$ ).

Continuing the work carried out in [8], in this paper we use a dielectrophoretic device to manipulate the trajectory of two different types of particles by using numerical simulations. The particles separated here are Circulating Tumor Cells and Red Blood Cells. We improve the mesh of the domain and experimentally validate the first step of the numerical simulation (the fluid mechanics part) and compare the results obtained in the numerical simulations obtained at different working frequencies.

## 2. Methods and materials

### A. Working principle - DEP

When the frequency of the electric field is low, the dielectrophoretic behavior of the cell is strongly influenced by extracellular factors, such as: types of protein tied on the membrane, cells dimension, the conductivity and the permittivity of the solution [9].

The dielectrophoretic force is described as the product between the real part of the Clausius–Mossotti factor, the cell radius,  $a$ , vacuum electrical permittivity,  $\varepsilon_0$ , suspension medium electrical permittivity,  $\varepsilon_M$ , and the square gradient of the electric field, as follows:

$$f_{DEP} = 2\pi a^3 \varepsilon_0 \varepsilon_M \text{Re}[CM] \nabla |\mathbf{E}|^2 \quad (1)$$

The complex Clausius–Mossotti factor is computed as follows [3]:

$$CM(\omega) = \frac{\varepsilon_P^* - \varepsilon_M^*}{\varepsilon_P^* + 2\varepsilon_M^*} \quad (2)$$

where  $\omega$  is the angular frequency,  $\varepsilon_P^*$  and  $\varepsilon_M^*$  are the complex permittivity of particle and medium, computed as:

$$\varepsilon_P^* = \varepsilon_P - j \frac{\sigma_P}{\omega} \quad (3)$$

$$\varepsilon_M^* = \varepsilon_M - j \frac{\sigma_M}{\omega} \quad (4)$$

where  $\sigma_P$  and  $\sigma_M$  are the conductivities of the particle and the medium.

In the region of high frequencies, the electric charge is changing the sign very fast, and the property that influences the cell movement is the conductivity.

### B. Dielectrophoretic device

The dielectrophoretic device was built on two layers, a base layer on pyrex glass that contains gold interdigitated electrodes and a second layer represented by the PDMS (polydimethylsiloxane) microchannel. The first substrate is fabricated on pyrex. The wafer is firstly cleansed by boiling in isopropyl alcohol. In the next step the negative photoresist MAN is developed with the mask of the interdigitated electrodes on the pyrex wafer. Over the wafer, a thin film of Cr/Au of 20/300 nm is deposited through electron beam deposition. Through the lift off process, the photoresist together with the two metals Cr/Au are removed from the glass substrate, while on the

wafer only the gold electrodes remain. The results of these procedures are presented in Fig. 1a. Subsequent, the wafer is cut into three parts, to obtain three devices.

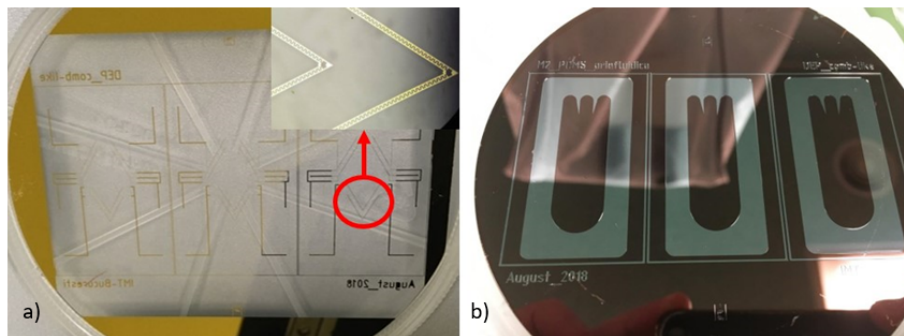


**Fig. 1.** a) Gold interdigitated electrodes on pyrex wafer; b) Si mold for PDMS obtained through DRIE.

To obtain the second substrate with the microfluidic channel, a mold is necessary. The mold is fabricated on a Si wafer. In the first step the Si wafer is cleaned in a solution of piranha followed by a thermal treatment. The positive photoresist AZ4562 is developed with the mask of the microchannel. The Si mold is obtained through DRIE by using the Bosch process for 38 minutes, Fig. 1 b.

The next step consists in the fabrication of the microfluidic channel in PDMS. The following quantity of 22 mL, base and curing agent, in ratio of 10:1 is prepared. The substance is mixed for five minutes until the mixture is homogeneous. The mixture is degassed using a desiccator for an hour. In the meantime, the microchannel mold is prepared in a small sealed chamber using 1 mL of chlorotrimethylsilane. The clear PDMS is poured over the microchannel mold and the whole compound is placed in the oven for an hour at 90 °C. The PDMS is peeled off the mold and punched in the zone of the microfluidic ports. The pyrex substrate along with the PDMS microchannel are placed inside RIE for surface activation and chemical bonding by using low power O<sub>2</sub> plasma, 20W. The two substrates are aligned and the PDMS is placed on top of the pyrex substrate, as it can be seen in Fig. 2. The tubing is attached using epoxy.

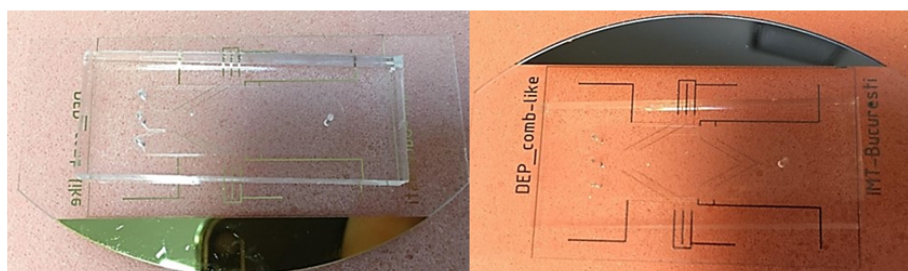


**Fig. 2.** Dielectrophoretic device.

The advantage of having the first substrate of pyrex glass is that the overall device is transparent, and more studies can be performed, such as PIV (particle image velocimetry) analysis.

Using this device in numerical simulations, two types of particles are separated: Circulating

Tumor Cells (CTCs) and Red Blood Cells (RBCs). The properties of the RBCs are well known from literature, and as CTCs we have chosen a single cellular line: MDA-MB-231 [10]. This CTC line is from the breast cancer and its peculiarity is that it has one of the smallest exterior diameters compared to other CTCs.

### 3. Numerical Methodology

The numerical simulations were performed using COMSOL Multiphysics [11]. To separate numerically particles in a suspension, several simplifications must be made since the required computational power is enormous. As such one simulation is split into three parts: laminar flow (for the suspension) – to determine the velocity and pressure fields, electric currents (for the electrodes) – to set up the electric field and particle trajectories, which has as initial solutions the first two steps.

A series of parameters is listed in Table 1, and alongside it we have the working fluid as a saline solution (PBS-phosphate buffered saline), and its properties are: density  $\rho_f = 1000 \text{ kg/m}^3$ , dynamic viscosity  $\eta_f = 1 \text{ mPa}\cdot\text{s}$ , conductivity  $\sigma_f = 2 \text{ S/m}$ , relative permittivity  $\varepsilon_f = 80$ .

**Table 1.** Numerical simulation parameters

<i>Parametername</i>	<b>Symbol</b>	<b>Value</b>	<b>Unit [S.I.]</b>
Frequency of the electric field	$f_0$	$10^5$	Hz
diameter: RBC	$d_{P1}$	$5 \cdot 10^{-6}$	m
diameter: CTC	$d_{P2}$	$12 \cdot 10^{-6}$	m
Particle conductivity: RBCs	$\sigma_{P1}$	0.31	S/m
Particle conductivity: CTC	$\sigma_{P2}$	0.62	S/m
Particle relative permittivity: RBC	$\varepsilon_{P1}$	59	-
Particle relative permittivity: CTC	$\varepsilon_{P2}$	130	-

Regarding the particles, further parameters are necessary for a better representation, such as: the density is considered  $\rho_p = 1050 \text{ kg/m}^3$ , the shell electrical conductivity  $\sigma_s = 1 \text{ }\mu\text{S/m}$ , the shell relative permittivity  $\varepsilon_s = 4.44$  and the shell thickness  $th_s = 9 \text{ nm}$ .

The geometry used in the numerical simulations is presented in Fig. 3 alongside a part of the boundary conditions. The microchannel has a length of 3 cm, a width of 1 cm and a height of  $50 \text{ }\mu\text{m}$ , one inlet and three outlets. The interdigitated electrodes have a length of  $20 \text{ }\mu\text{m}$  and a width of  $10 \text{ }\mu\text{m}$ . The mesh has 2.1 million elements with 0.88 the quality of the average element.

The interdigitated electrodes have a height of 300 nm, as such to reduce the computations, and as well the mesh, in the geometry they are considered surfaces. The mesh would have been very expensive if the scales in the geometry would have ranged from the nano scale to the millimeters scale. A symmetry plane was used to simplify the geometry along the x-axis.

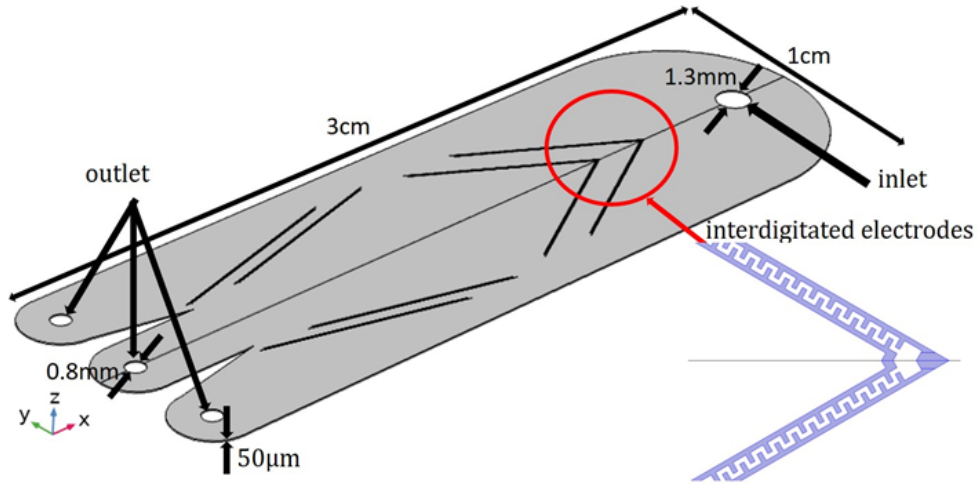


**Fig. 3.** Geometry of the dielectrophoretic device with a detail on the interdigitated electrodes.

In terms of boundary conditions, for the laminar flow, the inlet is set to velocity inlet and the outlets to pressure outlet, with the relative pressure set to 0. The walls of the geometry are set to no slip. The initial condition is represented by the value of the velocity at the inlet:  $v = 500 \mu\text{m/s}$ . The nondimensional number that characterizes the flow is the Reynolds number and we compute it with regards to the hydraulic diameter:

$$Re = \frac{\rho v D_h}{\eta} = 0.05 \quad (5)$$

$$D_h = \frac{4A}{P} = 98.8 \mu\text{m} \quad (6)$$

The Stokes approximation of the Navier-Stokes equations will describe the motion in our case, as the  $Re \ll 1$ :

$$\eta \Delta v = \nabla p \quad (7)$$

$$\nabla \cdot v = 0 \quad (8)$$

where  $v$  is the velocity vector and  $p$  is the pressure.

For the second step of the simulation, the electric field is modelled using the following equations:

$$\nabla \cdot J = Q_J \quad (9)$$

$$E = -\nabla V \quad (10)$$

$$D = \varepsilon_0 \varepsilon_r E \quad (11)$$

$$J = \sigma E + j\omega D + j_e \quad (12)$$

where  $E, Q_J, \omega, D, V, J_e$  are the electric field intensity, charge density, angular frequency, electric displacement field, electric potential and externally generated current density. The boundary conditions are represented by electrodes, which were given electric potential, while the rest of the device is insulated. On the exterior electrode, the applied electric potential is +5 V, and on the interior electrodes the applied electric potential is -5 V. The step is done in the frequency domain, and the frequency of the alternating electric field started from 100 kHz.

In the particle trajectories step, the first two module are embedded as initial solutions, in order to create an environment in which particles can be released and manipulated. The second law of Newton is the one that governs the trajectory of a particle:

$$m_p \frac{dv}{dt} = \sum F_{ext} \quad (13)$$

where the exterior forces that are acting on the particle, are in this case the drag force and the dielectrophoretic force. As we are in the laminar flowing regime and the particles are considered in the ideal case of a sphere, the drag force is given by Stokes:

$$F_D = 6\pi \eta_f r_{cel} V \quad (14)$$

where  $r_{cel}$  is the radius of a particle. The expression of the dielectrophoretic force is the one from Eq. (1).

## 4. Results

In the first numerical simulation, the input velocity is set to  $180 \mu\text{m/s}$ . This in turn will result in an average velocity of  $100 \mu\text{m/s}$  in the middle of the device, as it can be seen from the velocity contours in Fig. 4.

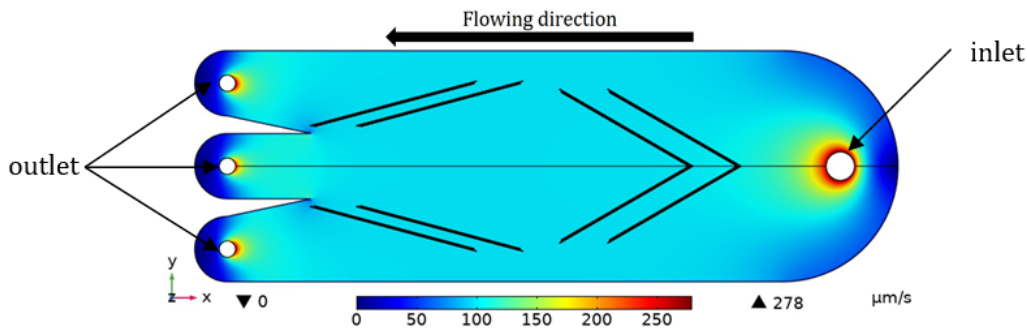
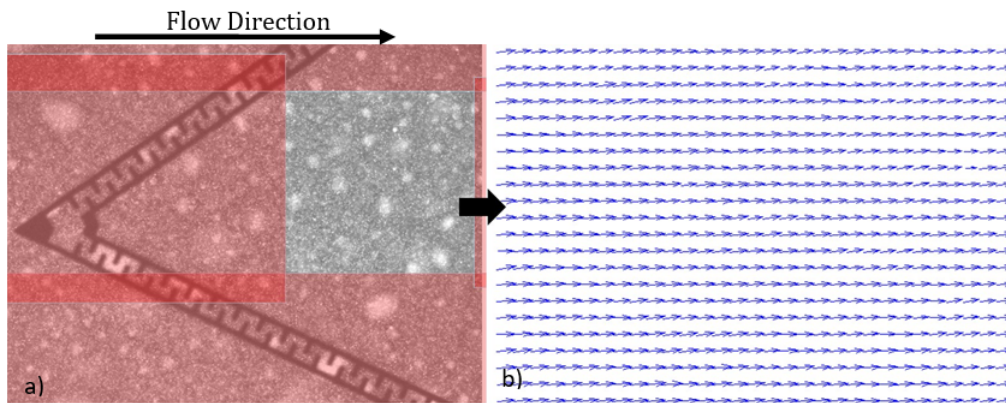


Fig. 4. Contours of velocity magnitude.

The  $\mu\text{PIV}$  technique was used to validate the velocity profile obtained numerically. The water was seeded with  $1 \mu\text{m}$  fluorescent particles in a concentration of 0.5%. A syringe pump was used to keep the flowrate constant, and the flowrate was set to  $375 \mu\text{L/hr}$ , which in turn will result in an average velocity of  $100 \mu\text{m/s}$ .



**Fig. 5.** a) Image acquisition (the flow is focused after the second row of electrodes; the electrodes are kept in sight for calibration) and b) postprocessing with adaptive PIV algorithm.

A small interrogation area was preferred for the computation of the velocity vectors in order to keep the errors at minimum. The vectors obtained are displayed in Fig. 5 b. The values of the velocity were taken on a perpendicular line to the flow field and the results are shown in Fig. 6 a.

When the conductivity of the medium is relatively high, the Clausius-Mossotti factor has the variation from Fig. 6 b over a wide range of frequencies. Under  $10^8$  Hz the Clausius-Mossotti factor is negative, which in turn results in a negative dielectrophoresis force and the particles will be driven towards the zone in the geometry with constant electric field. Over  $10^8$  Hz, the CTCs are recording a positive Clausius-Mossotti factor, that means that the dielectrophoretic force will be positive and the particles will be driven towards the zone in the geometry with high electric field gradients, such as close to the electrodes.

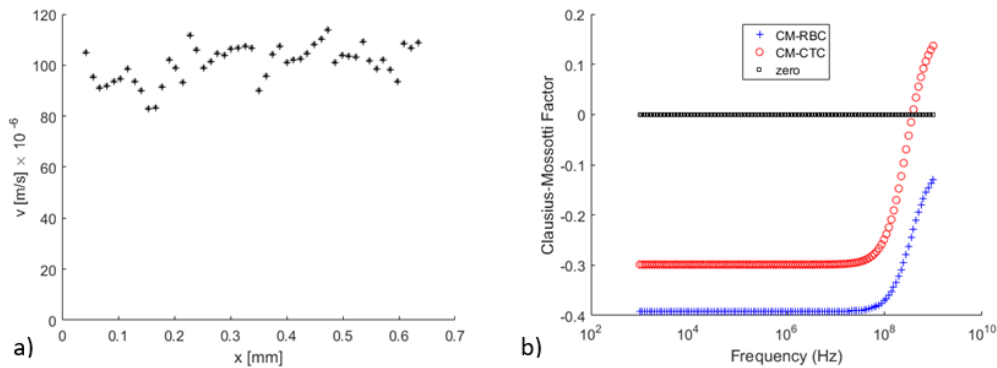


**Fig. 6.** a) Velocity distribution across a perpendicular line to the flow and b) CM factor for CTCs and RBCs.

For the next to numerical simulations, the initial velocity is raised to 500 m/s while two frequencies for the alternating electric field are used:  $10^5$  Hz and  $4.5 \cdot 10^8$  Hz. In both simulations, the electric potential and the electric field have the same distributions, as in Fig. 7. The highest

electrical field gradient is recorded between the electrodes and near the electrodes.

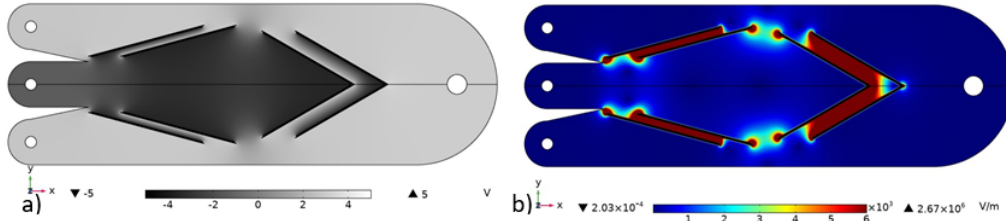


**Fig. 7.** a) Electric potential distribution b) Electric field distribution.

The difference between the two numerical simulations is displayed in Fig. 8. In the first simulation, with  $f = 10^5$  Hz Fig. 8 a, both particles are affected by negative dielectrophoresis and even at the last timestep,  $t = 300$  s, both particles remain attached to the electrodes. In the second simulation, with  $f = 4.5 \cdot 10^8$  Hz Fig. 8 b, the RBC is affected by negative dielectrophoresis while the CTC is affected by positive dielectrophoresis. The RBC passes through the zone of high electric field gradients and gets to its corresponding exit, while the CTC remains stuck on the electrode in the zone with high electric field gradients.

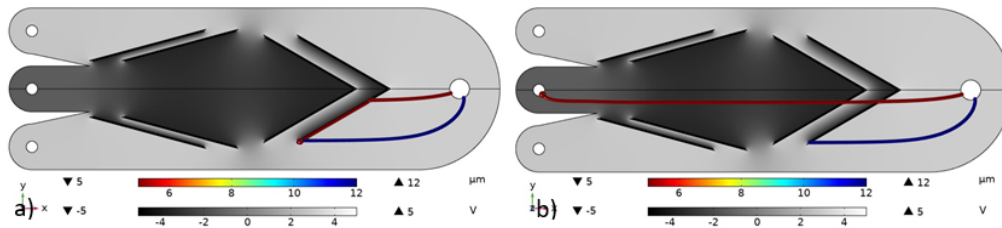


**Fig. 8.** Final particle trajectories a)  $t = 300$  s,  $f = 10^5$  Hz b)  $t = 273$  s,  $f = 4.5 \cdot 10^8$  Hz (red -RBC, blue-CTC).

## 5. Conclusions

The dielectrophoretic force was used to manipulate the particle trajectories inside a microchannel by performing 3D numerical simulations. At first the dielectrophoretic device is fabricated on two substrates, a glass substrate with gold interdigitated electrodes and the second substrate which consists in the PDMS microchannel. The device is tested experimentally using the  $\mu$ PIV technique and used to validate the numerical simulations (the fluid mechanics part). Two frequencies for the alternating electric field are tested, and the difference between them is that at  $10^5$  Hz, both particles are affected by negative dielectrophoresis, while at  $4.5 \cdot 10^8$  Hz the RBC is affected by negative dielectrophoresis while the CTC is affected by positive dielectrophoresis.

Better results are obtained in the case of using high frequencies. However, these high frequencies cannot really be obtained experimentally, except in the case of using very expensive

equipment and even so, there is a high probability that the cells will be damaged. As such simulations at 100 kHz can be improved either by changing the suspension medium or the electrode arrangement. It is important that the initial velocity is high, or in the range of 500  $\mu\text{m/s}$ . In turn the particle will gain enough inertial momentum to pass through the high electric field gradients and have its trajectory deviated towards its corresponding exit. A low velocity, and specially in experiment, will lead to a clogging of the device.

For future work, the experimental part can be extended by testing various types of cells, either CTCs or yeast cells, because to an extent they have the same electrical properties.

**Acknowledgements.** The work has been funded by the Operational Programme Human Capital of the Ministry of European Funds through the Financial Agreement 51675/09.07.2019, SMIS code 125125.

## References

- [1] MOON H. S., KWON K., KIM S. I., HAN H., SOHN J., LEE S., and JUNG H. I. Continuous separation of breast cancer cells from blood samples using multi-orifice flow fractionation (MOFF) and dielectrophoresis.
- [2] AGHAAMOO M., AGHILINEJAD A., CHEN X., and XU J., *On the design of deterministic dielectrophoresis for continuous separation of circulating tumor cells from peripheral blood cells*, *Electrophoresis* **40**(10), 2019, 1486–149.
- [3] PUNJIYA M., NEJAD H. R., MATHEWS J., et al., *A flow through device for simultaneous dielectrophoretic cell trapping and AC electroporation*, *Scientific Reports*, 9:11988, 2019.
- [4] AVRAM A., TIBEICĂC., MĂRCULESCU C., Volmer M., Avram M., Gavrilă H., *Bipolar magnetophoretic system for the manipulation of magnetic particles*, *U.P.B. Sci. Bull., Series C* **77**:171–180, 2015.
- [5] LENSCHOF A., AHMAD-TAJUDIN A., JARAS K., SWARD-NILSSON A.-M., ABERG L., MARKOVARGA G., MALM J., LILJA H., LAURELL T., *Acoustic whole blood plasmapheresis chip for prostate specific antigen microarray diagnostics*, *Analytical Chemistry* **81**(15):6030–6037, 2009.
- [6] WANG H.-Y., CHEN C.-Y., CHU P.-Y., ZHU Y.-X., HSIEH C.-H., LU J.-J., WU M.-H., *Application of an optically induced dielectrophoresis (odep)-based microfluidic system for the detection and isolation of bacteria with heterogeneity of antibiotic susceptibility*, *Sensors and Actuators B: Chemical* **307**:127540, 2020.
- [7] HUANG S. B., WU M. H., LIN Y. H., HSIEH C. H., YANG C. L., LIN H. C. and Lee, G. B., *High-purity and label-free isolation of circulating tumor cells (CTCs) in a microfluidic platform by using optically-induced-dielectrophoretic (ODEP) force*, *Lab on a Chip* **13**(7), 1371–1383, 2013.
- [8] CHIRIAC E., AVRAM M. and BĂLAN C., *Dielectrophoretic separation of Circulating Tumor Cells and Red Blood Cells in a microfluidic device*, 2020 International Semiconductor Conference (CAS), pp. 211–214.
- [9] SONKER M., KIM D., EGATZ-GOMEZ A., ROS A., *Separation Phenomena in Tailored Micro- and Nanofluidic Environments*, *Annual Review of Analytical Chemistry* **12**(1), 475–500, 2019.
- [10] TRUONGVO T. N., KENNEDY R. M., CHEN H., CHEN A., BERNDT A., Agarwal M., Zhu L., Nakshatri H., Wallace J., Na S., Yokota H., Ryu J. E., *Microfluidic channel for characterizing normal and breast cancer cells*, *Journal of Micromechanics and Microengineering* **27**(3): 035017, 2017.
- [11] COMSOL Multiphysics Reference Manual, 2019.